Ordered Structure in Blends of Block Copolymers. 1. Miscibility Criterion for Lamellar Block Copolymers†

Takeji Hashimoto,* Komei Yamasaki,‡ Satoshi Koizumi, and Hirokazu Hasegawa

Department of Polymer Chemistry, Faculty of Engineering, Kyoto University, Kyoto 606, Japan

Received November 16, 1992; Revised Manuscript Received February 16, 1993

ABSTRACT: Morphology of binary mixtures of poly(styrene-*block*-isoprene) (SI) having different compositions f_{PS} of the polystyrene block in SI and total molecular weights was investigated on the solution-cast film with toluene as a neutrally good solvent. In the range of the composition f_{PS} = 0.35–0.69 covered, the two SI copolymers were found to be totally miscible on the molecular level at all compositions, forming a single microdomain morphology, if their molecular weight ratio is smaller than about 5. They were found to be only partially miscible, if their molecular weight ratio is greater than about 10, forming macroscopically phase-separated coexisting lamellar microdomains with different domain spacings. In the partially miscible pairs, the copolymer with the larger molecular weight was found to solubilize the copolymer with the smaller molecular weight up to about 30 wt %, but the copolymer with the smaller molecular weight was found to hardly solubilize the copolymer with a larger molecular weight. A new but unidentified bicontinuous ordered microdomain structure was found for a miscible pair.

I. Introduction

Many reports have been presented on phase transitions, self-assembly, and ordered structures in the segregation limit for mixtures of A–B type diblock (or A–B–A type triblock) copolymers with A and/or B homopolymers.[1-20] There are some reports which further extended the study along this line to that for mixtures of block copolymers and C homopolymers.[21-25] In this series of work, we further extended the studies along this line to a new system composed of binary mixtures of A–B diblock copolymers with different compositions and molecular weights and aimed to study their self-assembling processes and mechanisms in the solution-cast process and their ordered structures. To simplify our experimental condition, we dealt with the solution-cast process with a neutrally good solvent.

One may realize that the self-assembly of the binary mixtures of two block copolymers, e.g., A_1–B_2/A_3–B_4, in a segregation limit involves a new problem, by comparing with that of an A–B diblock copolymer and an A homopolymer, e.g., A_1–B_2/A_3, where A_i and B_i are the A and B block chains with molecular weight M_i. In A_1–B_2/A_3–B_4, one end (i.e., chemical junction) of A_1 and A_3 block chains must be confined somewhere close to the interface between A and B microdomains, and the block chains must be packed in A-microdomain space, keeping the demand of incompressibility (i.e., the total segment density is constant everywhere in domain space), while in A_1–B_2/A_3, or A_1–B_2/C, the two chain ends of A_3 or C are not confined to the interface, having a greater translational entropy (freedom) in the direction normal to the interface than A_3 in A_3–B_4 block chains. Since this translational entropy becomes trivial in A_1–B_2/A_3–B_4, a contribution of the *elastic free energy of stretching* to the net free energy of the system becomes essentially important. This new aspect of the enhanced elastic contribution should be highlighted in our problem here. It should be noted that our problem may come across recent theoretical developments[26,27] on structures and properties of planar grafted layers. It should be also noted that there are some earlier works which dealt with microdomain formation of A_1–B_2/A_3–B_4 systems in the regime of two copolymers being totally miscible in the microdomains.[28,29]

The self-assembly of A_1–B_2/A_3–B_4 involves an interplay of macrophase and microphase separation as in that of A_1–B_2/A_3, A_1–B_2/C, etc.[8,23-25,30] In the context of mean-

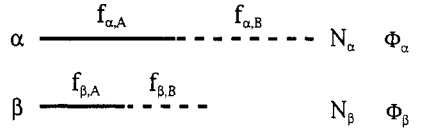

Figure 1. Schematic diagram indicating the molecular parameters for the binary mixtures of block copolymers. The parameters $f_{K,J}$ (K = α, β, J = A, B), N_K (K = α, β), and Φ_K (K = α, β) designate the volume fraction of the Jth chain in the Kth block copolymer, number-average degree of polymerization of the Kth block copolymer, and composition of the Kth block copolymer in a mixture, respectively.

Table I. Molecular Characteristics of Block Copolymers

specimen code	$M_n \times 10^{-3}$ [a]	S/I[b] wt %	S/I[b] vol %	M_w/M_n[c]	morphology
HK-7	31.9	35/65	32/68	1.09	lamella
HK-17	8.5	50/50	46/54	1.25	disorder
HS-9	1030	52/48	48/52	1.62	lamella
HS-10	81.4	63/37	60/40	1.13	lamella
HY-8	31.6	48/52	44/56	1.07	lamella
HY-10	164	69/31	66/34	1.17	tetrapod
HY-12	534	49/51	45/55	1.16	lamella

[a] Osmometry. [b] Mass analysis. [c] GPC.

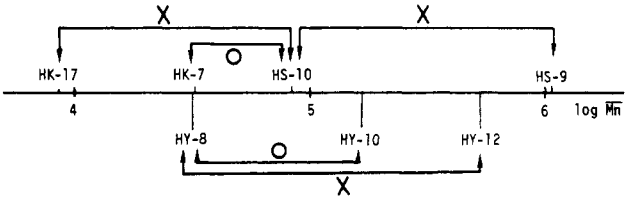

Figure 2. Schematic diagram showing the pairs of the A–B block copolymers in the mixtures studied in this work. The number-average molecular weight of the copolymers is indicated in a logarithmic scale. The symbols ○ and × mean the miscibility at all compositions and partial miscibility, respectively.

† Presented in part at the 32nd Symposium of the Society of Polymer Science, Japan, Oct 1983. *Polym. Prepr. Jpn., Soc. Polym. Sci., Jpn.* **1983**, *32*, 1687–1694.

‡ Present address: Polymer Research Laboratory, Idemitsu Petrochemical Co., Ltd., Anegasaki, Ichihara, Chiba 299-01, Japan.

0024-9297/93/2226-2895$04.00/0

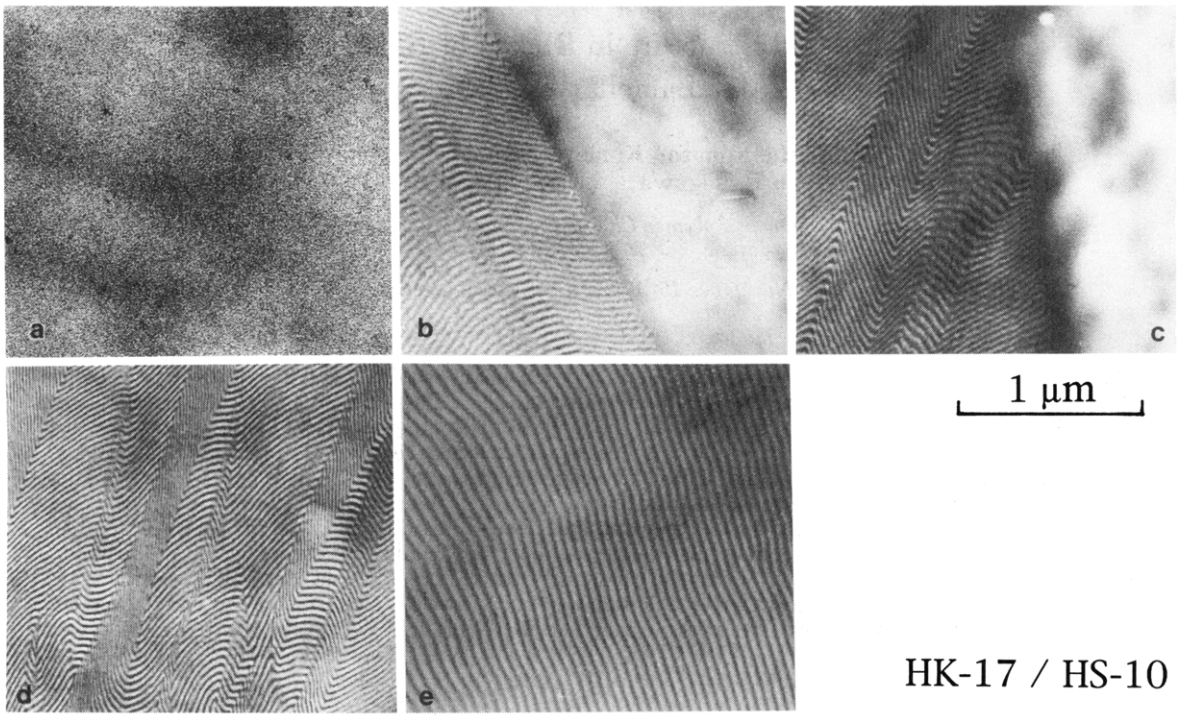

Figure 3. Transmission electron micrographs of ultrathin sections of HK-17/HS-10 binary mixtures stained by osmium tetraoxide with compositions (wt %/wt %) (a) 100/0, (b) 80/20, (c) 50/50, (d) 20/80, and (e) 0/100. These mixtures show partial miscibility, forming coexisting macrophases (b and c).

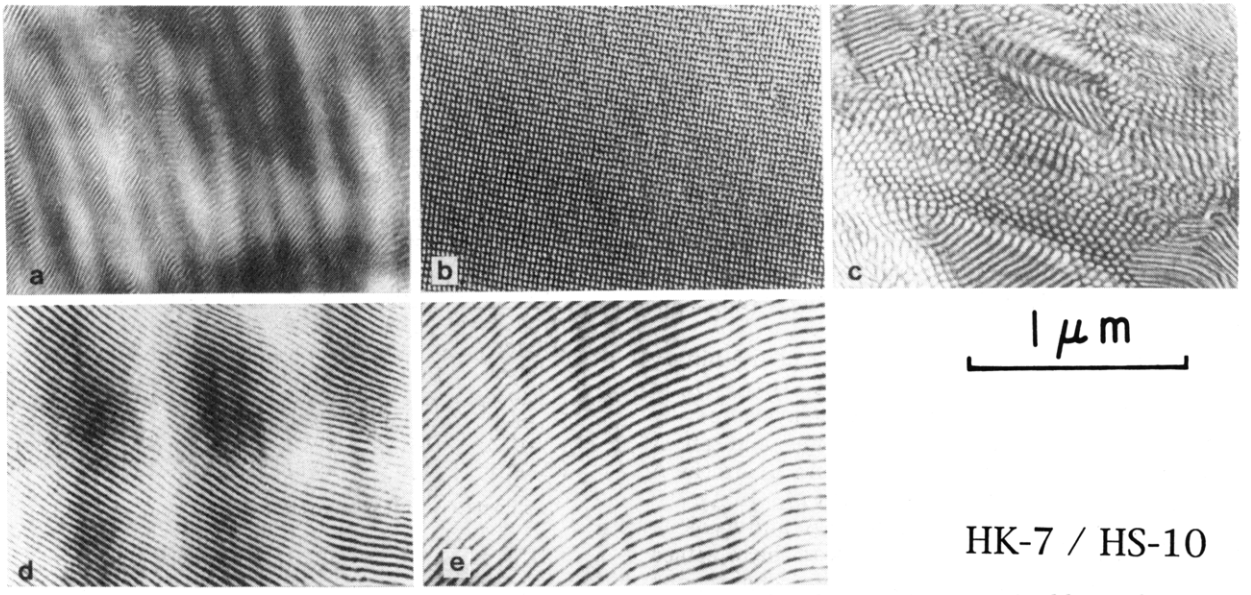

Figure 4. Transmission electron micrographs of ultrathin sections of HK-7/HS-10 binary mixtures stained by osmium tetraoxide with compositions (wt %/wt %) (a) 100/0, (b) 80/20, (c) 50/50, (d) 20/80, and (e) 0/100. These mixtures show the complete miscibility at all compositions (from b to d).

field theory, the spinodal point for the macrophase transition between single-phase disordered copolymers and two-phase but still disordered copolymers can be predicted by

$$\chi_{\mathrm{eff,s}} = 1/N_\alpha\Phi_\alpha + 1/N_\beta(1-\Phi_\alpha) \tag{1}$$

$$\chi_{\mathrm{eff}} = (f_{\alpha,\mathrm{A}} - f_{\beta,\mathrm{A}})^2\chi_{\mathrm{AB}} \tag{2}$$

where χ_{eff} is the Flory segmental interaction parameter between the two polymers per monomer base, $\chi_{\mathrm{eff,s}}$ is the χ_{eff} value at the spinodal point, and other quantities will be defined in the next paragraph. Among the five mixtures of two copolymers studied here, the mixture having the largest mismatch in the composition has $(f_{\alpha,\mathrm{A}} - f_{\beta,\mathrm{A}})^2 = 0.28^2 \cong 0.08$. This makes $\chi_{\mathrm{eff}} < \chi_{\mathrm{eff,s}}$ for all the systems covered here, which simplifies our problem on the self-assembly such that the macrophase separation between the disordered copolymers is not expected to occur.

We define here one of the two block copolymers having the larger molecular weight as α and the other copolymer having the smaller molecular weight as β (Figure 1). Then the molecular parameters characterizing the mixtures are $f_{\alpha,\mathrm{A}}$, $f_{\beta,\mathrm{A}}$, N_α, and N_β and their environmental parameters are p, T, Φ_α, and c, where $f_{K,\mathrm{A}}$ is the composition of A block chain in the Kth A–B copolymer defined by

$$f_{K,\mathrm{A}} = N_{K,\mathrm{A}}/N_K \ (K = \alpha \text{ or } \beta) \tag{3}$$

$$N_K = N_{K,\mathrm{A}} + N_{K,\mathrm{B}} \ (K = \alpha \text{ or } \beta) \tag{4}$$

with $N_{K,J}$ being the degree of polymerization (DP) of the

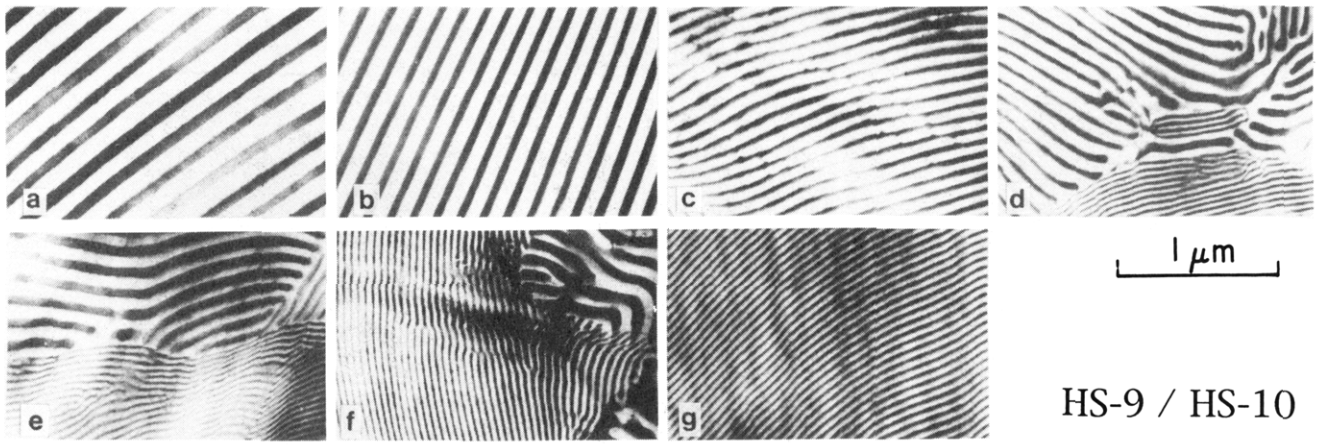

Figure 5. Transmission electron micrographs of ultrathin sections of HS-9/HS-10 binary mixtures stained by osmium tetraoxide with compositions (wt %/wt %) (a) 100/0, (b) 90/10, (c) 80/20, (d) 70/30, (e) 50/50, (f) 20/80, and (g) 0/100. The micrographs d–f show coexisting macroscopic domains of different lamellar identity periods.

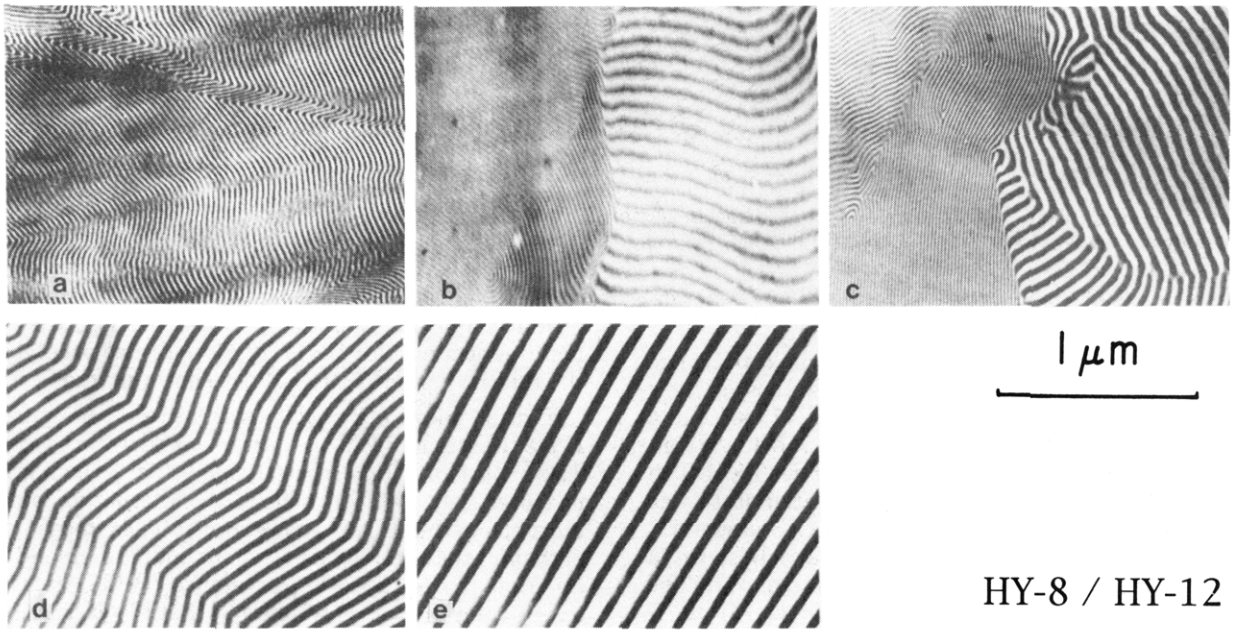

Figure 6. Transmission electron micrographs of ultrathin sections of HY-8/HY-12 binary mixtures stained by osmium tetraoxide with compositions (wt %/wt %) (a) 100/0, (b) 80/20, (c) 50/50, (d) 20/80, and (e) 0/100. The micrographs b and c show coexisting macroscopic domains of different identity periods.

Jth block chain (J = A or B) in the Kth copolymer, N_K is the total DP of the Kth copolymer, p is the pressure, T is the absolute temperature, Φ_K is the volume fraction of the Kth copolymer in the mixtures ($\Phi_\beta = 1 - \Phi_\alpha$), and c is the concentration of polymers α and β in the solution, if solvent exists in the system.

II. Experimental Methods

A. Samples. A series of poly(styrene-*block*-isoprene) diblock copolymers (SI) were prepared using a living anionic polymerization method. Their molecular characteristics and the specimen codes are listed in Table I. Binary mixtures of the SI copolymers studied are shown in Figure 2 where each copolymer is placed along the axis indicating its total number-average molecular weight in a logarithmic scale. The mixtures HK-7/HS-10 and HY-8/HY-10, marked by circles, were found to be miscible at all compositions (except for HY-8/HY-10 (80/20, wt %/wt %)) but the mixtures HK-17/HS-10, HS-10/HS-9, and HY-8/HY-12 marked by the symbol × were found to be only partially miscible, as will be shown later.

All the mixtures were first dissolved into dilute solutions with toluene as a neutrally good solvent in which two copolymers were molecularly mixed in the disordered state. The solutions were then concentrated to about 5 wt % of the total polymers by slowly evaporating the solvent. The solutions were then cast into film specimens of about 0.5 mm thick by slowly evaporating the solvent at 30 °C over 10 days. The cast films were further dried in a vacuum oven controlled at 120 °C for 5 h prior to investigation by transmission electron microscopy (TEM) and small-angle X-ray scattering (SAXS).

B. TEM. The microdomain structures formed in binary mixtures were examined by transmission electron microscopy (TEM). For this purpose, the cast films were first stained by osmium tetraoxide vapor, and then ultrathin sections of ca. 50 nm thick were obtained by using an ultramicrotome (LKB 4800A Ultrotome) with a glass knife. The ultrathin sections on electron microscope grids were further stained by exposure to osmium tetraoxide vapor for a few hours. Electron microscopic observation was done with a Hitachi H-600 transmission electron microscope operated at 100 kV.

C. SAXS. The microdomain structures were investigated by SAXS using a Rigaku rotating-anode X-ray generator operated at 50 kV and 200 mA (wavelength $\lambda = 0.154$ nm). SAXS profiles were corrected for air scattering, absorption, and background scattering due to thermal diffuse scattering (TDS).[31] The absolute intensity was measured by the nickel foil method,[32] although it is not important in this study.

III. Experimental Results

A. TEM Studies. Figures 3–7 summarize the results of our TEM studies in which morphologies formed in the

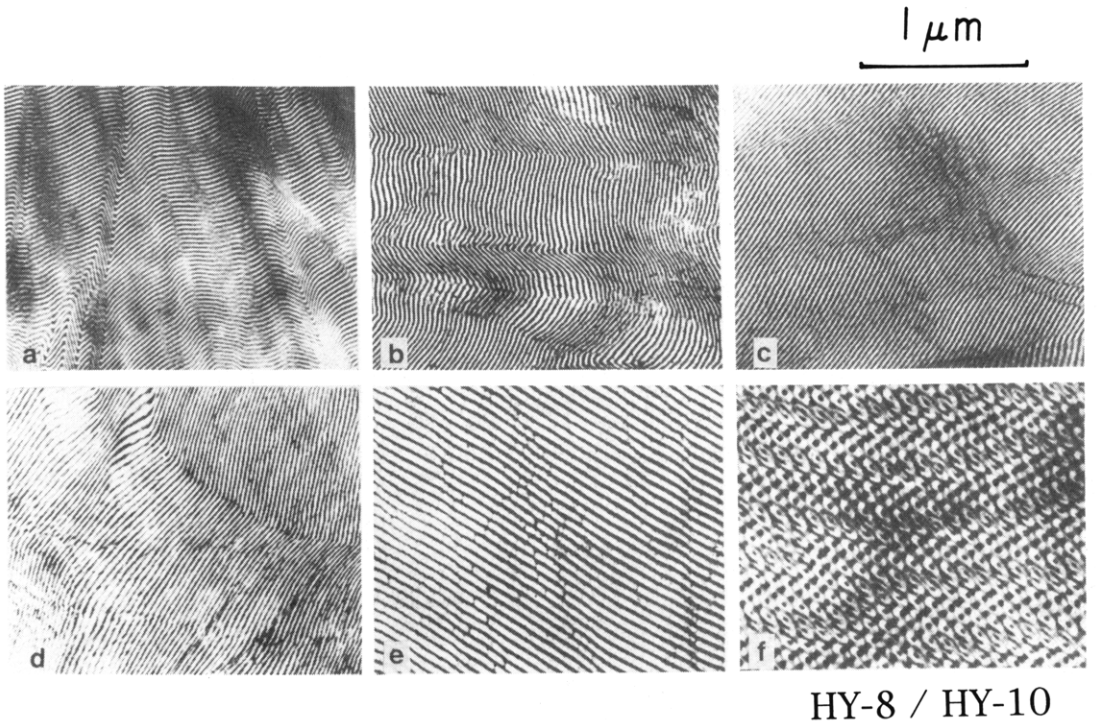

Figure 7. Transmission electron micrographs of ultrathin sections of HY-8/HY-10 binary mixtures stained by osmium tetraoxide with compositions (wt %/wt %) (a) 100/0, (b) 80/20, (c) 60/40, (d) 50/50, (e) 20/80, and (f) 0/100.

film specimens of each mixture were shown as a function of composition.

Figure 3 shows the morphologies of the pure copolymers HK-17 (part a) and HS-10 (part e) as well as those of their mixtures (parts b–d). The copolymer HK-17 has such a low molecular weight that it exists only in the disordered state, showing a featureless morphology under TEM. The fact that the copolymer is in the disordered state was previously proven by the quantitative SAXS analysis.[33] The 20/80 mixture of HK-17/HS-10 (part d) shows a regular alternating lamellar microdomain morphology composed of polystyrene (PS) and polyisoprene (PI) lamellae with a single identity period D which depends on the composition Φ_α. However, the mixtures HK-17/HS-10 80/20 (part b) and 50/50 (part c) show macroscopic phase separation into the domain composed of the alternating PS and PI lamellae and the domain composed of disordered HK-17. The identity period D of the lamellae phase seems to depend generally on Φ_α which will be discussed in section III. B.

Figure 4 shows morphologies of pure block copolymers of HK-7 (part a) and HS-10 (part e) and their 80/20 (part b), 50/50 (part c), and 20/80 mixtures (part d). Pure copolymers as well as the 20/80 mixture show the lamellar morphology of a single, composition-dependent identity period of D. To our big surprise, the 80/20 and 50/50 mixtures, however, do not exhibit the lamellar microdomains, despite the fact that their constituent copolymers show the lamellar morphology. They show rather uniform, ordered, bicontinuous microdomain structures whose structure symmetry remains unidentified at present. The details of their morphologies will be described elsewhere.[34]

Figure 5 shows morphologies of neat copolymers HS-9 (part a) and HS-10 (part g) as well as those of their 90/10 (part b), 80/20 (part c), 70/30 (part d), 50/50 (part e), and 20/80 mixtures (part f). The neat copolymers as well as the 90/10 and 80/20 mixtures show the alternating lamellar morphology with a single, composition-dependent identity period D. The mixtures 70/30, 50/50, and 20/80 also show only the lamellar morphology, but they show a macroscopic phase separation into the two macroscopic domains having different lamellar identity periods. Almost the same features as found for HS-9/HS-10 were also observed for the mixtures of HY-8/HY-12, as shown in Figure 6.

Figure 7 shows morphologies of the neat copolymers of HY-8 (part a) and HY-10 (part f) as well as those of their 80/20 (part b), 60/40 (part c), 50/50 (part d), and 20/80 mixtures (part e). HY-8 shows the alternating lamellar morphology, but HY-10 shows one of a TEM image typical of that for the ordered bicontinuous double diamond built up from the tetrapod-like structure (OBDD–tetrapod) entity composed of polyisoprene (PI) block chains, the detailed discussion of which was given elsewhere.[35,36] All the binary mixtures of the copolymers studied in this experiment uniformly exhibit the lamellar morphology of a single, composition-dependent identity period.

B. SAXS Studies. SAXS results corresponding to the TEM results shown in Figures 3–7 were presented in Figures 8–12, respectively. In Figure 8, HK-17 shows a very broad scattering maximum marked by the thick arrow, corresponding to the wavelength of the dominant mode of the concentration fluctuations in the single-phase state.[33] On the other hand, HS-10 shows multiple-order diffraction maxima at the positions of integer multiples of that of the first-order scattering maximum, the profile of which is relevant to the alternating lamellar morphology. The fifth-order diffraction peak is suppressed due to the volume fraction of one of the domains (the PI domain in this case) being close to 40%. The 20/80 mixture shows the profile relevant to the lamellar morphology with its identity period smaller than that for HS-10, as shown in the larger-angle shift of the corresponding diffraction maxima marked by thin arrows, consistent with the TEM result shown in Figure 3. The 80/20 mixture, however, clearly shows the profile comprising that from regions having alternating lamellar morphology which gives rise to the diffraction maxima marked by the thin arrows and that from the regions having a disordered single-phase state which gives rise to a scattering maximum shown by a thick arrow. The profile for the 50/50 mixture is found to be similar to that

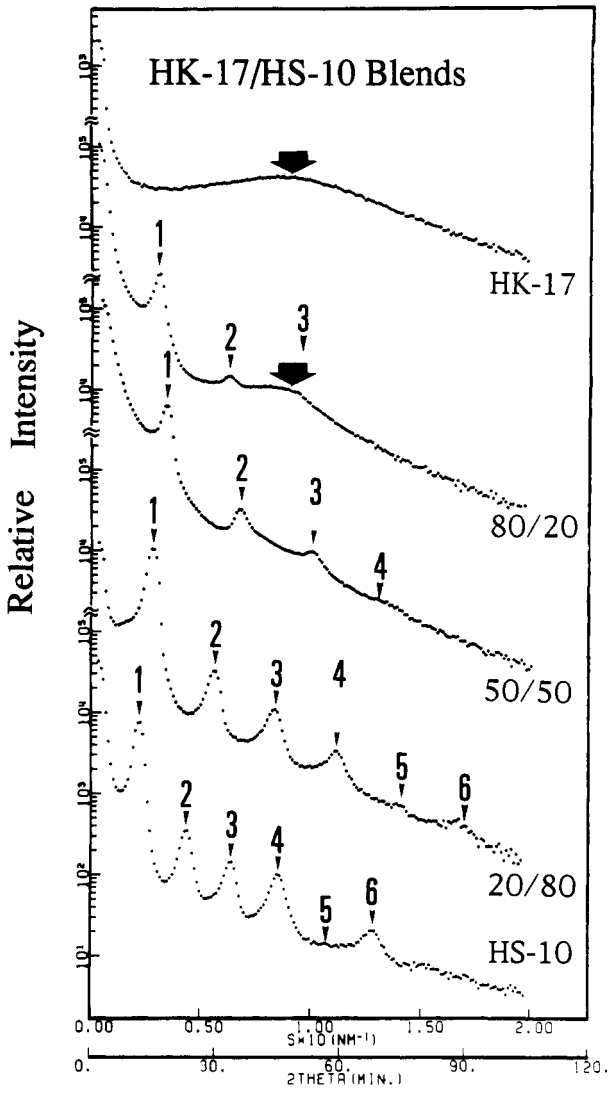

Figure 8. SAXS profiles obtained for the binary mixtures of HK-17/HS-10 with compositions of 100/0 (wt %/wt %), 80/20, 50/50, 20/80, and 0/100. Pure HK-17 and the mixture 80/20 show a broad scattering maximum due to the dominant mode of the concentration fluctuation in the single-phase state for HK-17 (thick arrow).

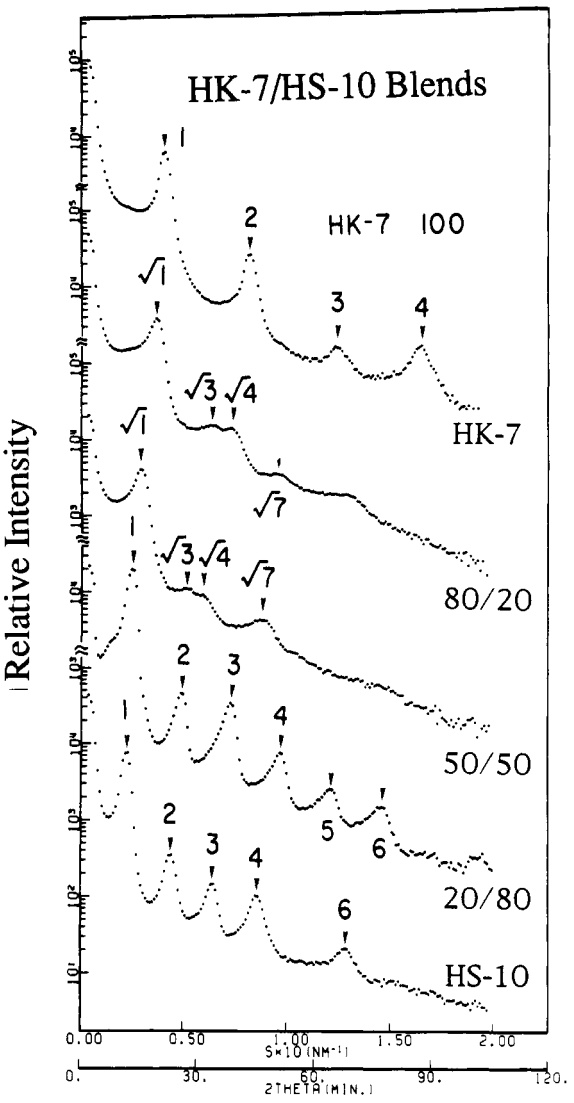

Figure 9. SAXS profiles obtained for the binary mixtures of HK-7/HS-10 with compositions of 100/0 (wt %/wt %), 80/20, 50/50, 20/80, and 0/100. Pure HK-7, pure HS-10, and the mixture 20/80 show typical scattering profiles for lamellar morphology, while the mixtures 80/20 and 50/50 show profiles with hexagonal symmetry.

for the 80/20 mixture after a quantitative intensity analysis based upon a paracrystal model, although the details will not be discussed here.

Figure 9 shows the SAXS profiles for HK-7/HS-10. Neat copolymers HK-7, HS-10, and their 20/80 mixture show clearly the profiles relevant to the lamellar morphology with a long-range spatial order. The 80/20 and 50/50 mixtures which exhibit the unique TEM micrographs of the ordered bicontinuous microdomain morphology show the profiles which are very different from the lamellar morphology. The profiles are apparently similar to those for hexagonally packed cylinders or the spherical domains with a cubic symmetry, the detailed analyses of which are, however, beyond the scope of this work.

Figure 10 shows SAXS profiles for HS-9/HS-10. All the mixtures show the profiles relevant to the lamellar morphology, consistent with the TEM micrographs in Figure 5, although the lamellar morphology is less clear from the SAXS profiles of the 90/10, 80/20, and 70/30 mixtures. Using the information obtained by the TEM studies, the SAXS profiles can be interpreted as follows. The diffraction maxima from the lamellar microdomains of the neat copolymer HS-9 or those from grains of lamellae rich in HS-9 for the mixtures are marked by arrows with numbers in circles. The diffraction maxima from the lamellae of the neat copolymer HS-10 or those from grains of the lamellae rich in HS-10 are marked by arrows with numbers without circles. The integer number attached to each arrow corresponds to the order of the diffraction from the respective lamellar domains.

Figure 11 shows the SAXS profiles for HY-8 and HY-12 where the orders of the diffraction maxima from each grain of HY-8 or HY-12 are respectively indicted by thick arrows with numbers in circles and thin arrows with numbers without circles, with the integer numbers corresponding to the order of diffractions, as in Figure 10.

Figure 12 shows the SAXS profiles for HY-8 and HY-10 where the assignment of the diffraction maxima of each profile was given in a manner similar to that of Figures 10 and 11. Here the following remarks are worth noting: (i) only HY-10 shows the profile relevant to the OBDD-tetrapod network,[35,36] but all other profiles are those relevant to the lamellar morphology; (ii) only the 80/20 mixture shows the maxima relevant to the coexisting macrophases rich in HY-10 (the maxima marked by thin arrows) and rich in HY-8 (the maxima marked by thick arrows with numbers in circles), but all other specimens show the profiles from a single morphological entity (either the lamella or OBDD–tetrapod network).

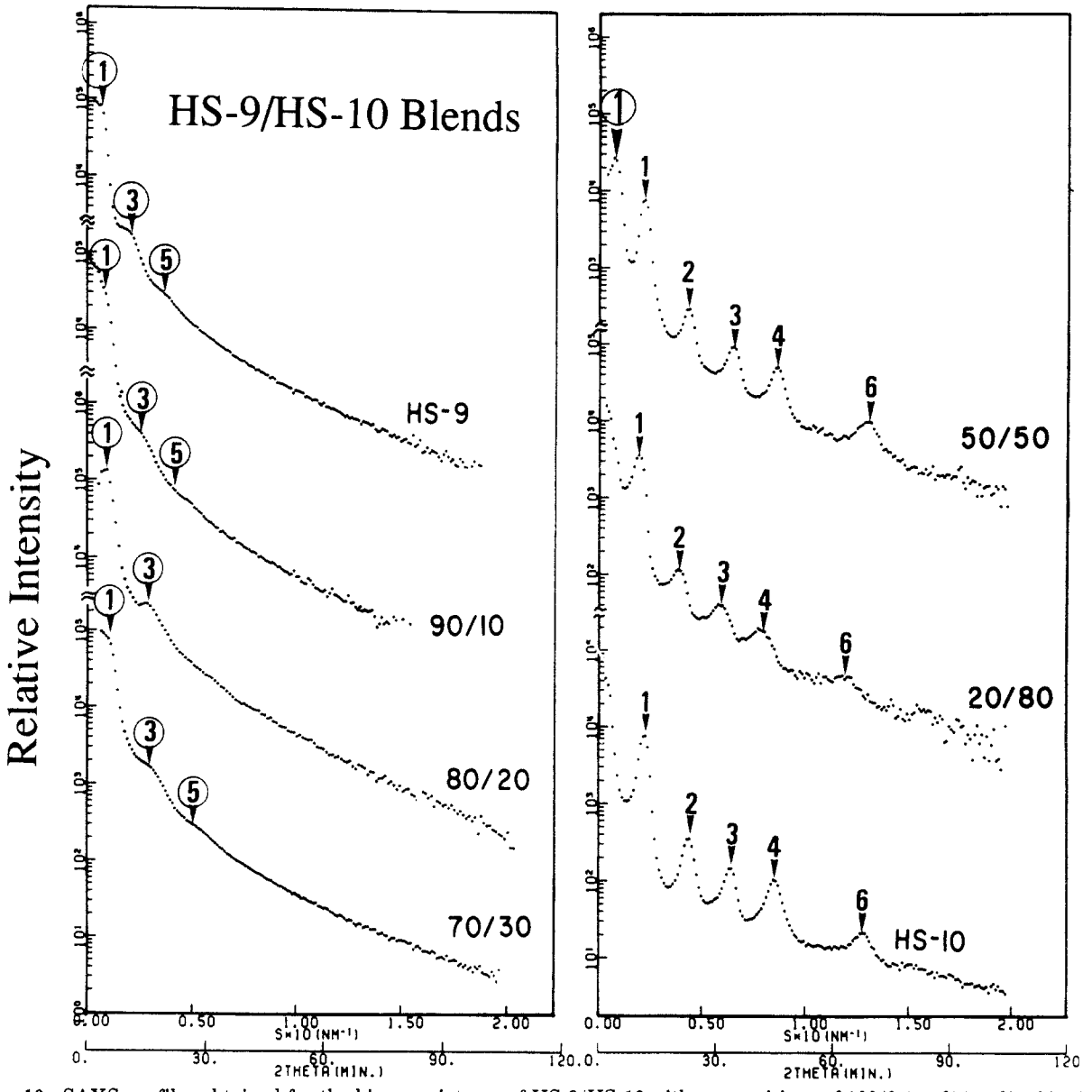

Figure 10. SAXS profiles obtained for the binary mixtures of HS-9/HS-10 with compositions of 100/0 (wt %/wt %), 90/10, 80/20, 70/30, and 50/50, 20/80, and 0/100. Scattering maxima and shoulders due to the lamellae rich in HS-9 are indicated by numbers with circles, while the other peaks indicated by numbers without circles are due to the lamellae rich in HS-10. The number indicates the order of diffraction.

IV. Discussion

A. Miscible Blends. The TEM and SAXS results show that the HK-7/HS-10 mixtures are miscible at all compositions, forming a single microdomain morphology. Almost the same result was obtained for HY-8/HY-10 except for the 80/20 mixture. Here we discuss how the domain spacing depends on the composition of the mixtures in the regime where the two copolymers α and β are miscible on the molecular level and form a single domain morphology. Parts a and b of Figure 13 show the domain spacing D as a function of the compositions of the large molecular weight copolymer α (HS-10 and HY-10, respectively). The figures also include the scale of number-average molecular weight M_n of the two mixtures α and β

$$M_n = x_\alpha M_{n,\alpha} + x_\beta M_{n,\beta} \tag{5}$$

where $M_{n,K}$ ($K = \alpha$ or β) is the number-average molecular weight of the Kth component and x_K is the mole fraction of the Kth component ($x_\alpha + x_\beta = 1$).

Figure 13a shows that the spacing D changes continuously with Φ_α, the volume fraction of the large molecular weight copolymer. The abscissa actually represents weight fraction, instead of Φ_α. We hereafter ignore the minor difference between volume and weight fraction. The solid line is the value D calculated on the basis of an extended Helfand–Wassermann theory[37] in which the value D for the mixture is assumed to be identical to the value D for a lamellar morphology of the neat copolymer having the corresponding M_n. Figure 13b also shows a continuous change of D with Φ_α, except for $\Phi_\alpha = 0.2$ where the two lamellar regions having the spacing close to each other coexist. Thus we can conclude that the mixtures of the SI copolymer with

$$N_\alpha/N_\beta < 5 \tag{6}$$

can be molecularly mixed at all compositions to form a single microdomain morphology. This conclusion confirms our earlier results.[28,29]

We previously reported[29] that the domain spacing D of the mitures α and β in the molecularly miscible regime can be scaled with M_n by

$$D \sim M_n^{2/3} \tag{7}$$

This postulate was tested in Figure 14 for our mixtures where the values D for all the miscible mixtures exhibiting

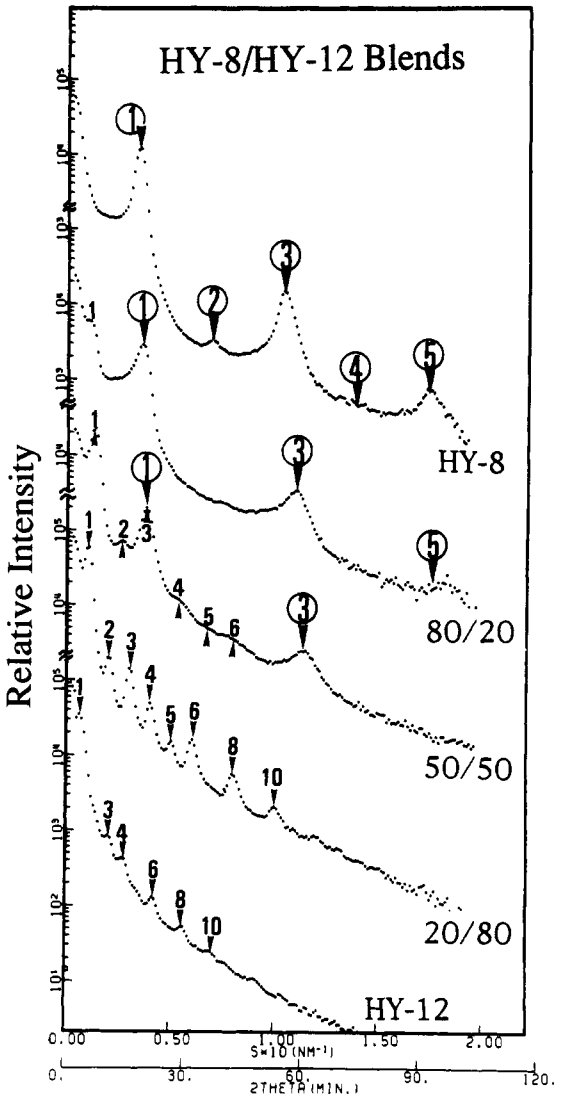

Figure 11. SAXS profiles obtained for the binary mixtures of HY-8/HY-12 with compositions of 100/0 (wt %/wt %), 80/20, 50/50, 20/80, and 0/100. Scattering peaks due to the lamellae rich in HY-8 are indicated by numbers with circles, while the other peaks and shoulders indicated by numbers without circles are due to the lamellae rich in HY-12. The number indicates the order of diffraction.

a single morphology are plotted as a function of M_n in a double-logarithmic scale. The result is seen to be consistent with the 2/3 power law, except for the highest molecular weight limit (obtained for HS-9), for which D is much less than the predicted value. The suppression of D may be due to the nonequilibrium effect previously discussed.[38]

Next, we discuss the morphological changes observed (in Figures 4 and 7) upon mixing the copolymers with different compositions. Parts a and b of Figure 4 reveal that the mixing of a small amount of the PS-rich copolymer HS-10 into the majority of the PI-rich copolymer HK-7 has obviously changed the inteface curvature, forming the new ordered bicontinuous morphology. With a further decrease of the PS volume fraction in the copolymer, denoted hereafter f_{PS}, HK-7 is expected to have an interface with a concave curvature toward the centers of the PS microdomains, so that its Gaussian curvature of the interface $K \equiv k_1k_2$ may satisfy $K \geq 0$, i.e., the criterion for the ellipsoidal ($K > 0$) and paraboloidal interfaces ($K = 0$), where k_1 and k_2 are the principal curvatures of the interface. Upon adding the copolymer HS-10 with $f_{PS} = 0.60$, i.e., with the composition approximately opposite to that of HK-7, this interface curvature may be altered to the hyperboloidal interface characterized by a negative Gaussian curvature $K = k_1k_2 < 0$. This hyperboloidal interface is responsible for the ordered bicontinuous morphology in 3D space. It is interesting to note that the solubilization of the small amount of HS-10 is sufficient to alter the interface curvature of the major component HK-7 of the mixture, *giving a curvature-driven morphological transition.*

Upon comparing parts e and f of Figure 7, it is very impressive to note that a small amount of HY-8 with $f_{PS} = 0.44$ solubilized into the OBDD phase of HY-10 with $f_{PS} = 0.66$ has changed the interface curvature of HY-10 from the hyperboloidal interface found in the OBDD–tetrapod microdomains to the paraboloidal interface found in the lamellar microdomains. Thus we can find again that a minority copolymer can control or change the interface curvature of a major copolymer in the case where the constituent block chains of the minority copolymer are solubilized into the respective domains of the majority copolymers with their chemical junctions near the interface of the coexisting domains. This curvature change causes the morphological transition between lamella and OBDD–terapod.

B. Immiscible Blends. Parts a–c of Figure 15 show the spacing D as a function of Φ_α for HK-17/HS-10, HS-10/HS-9, and HY-8/HY-12, respectively. These are the mixtures which show only a partial miscibility. All the mixtures are found to be miscible in the composition range of

$$\Phi_\alpha < \Phi_{\alpha,CS} \text{ and } \Phi_\alpha > \Phi_{\alpha,CL} \quad (8)$$

forming a single microdomain morphology but immiscible in the composition range of

$$\Phi_{\alpha,CS} < \Phi_\alpha < \Phi_{\alpha,CL} \cong 0.7 \quad (9)$$

forming the two coexisting macrophases of the lamellae with large and small spacings, i.e., D_α and D_β respectively. All the mixtures show that

$$1 - \Phi_{\alpha,CL} = \Phi_{\beta,CL} \gg \Phi_{\alpha,CS} \quad (10)$$

That is, the larger molecular weight copolymer α can solubilize a greater amount of the smaller molecular weight copolymer β in its microdomains than β can solubilize α in its microdomains, although the exact criteria of solubilization $\Phi_{\alpha,CS}$ and $\Phi_{\alpha,CL}$ have not been assessed yet. No experimental data were obtained so far at small Φ_α, and the broken lines drawn in the region $0 < \Phi_\alpha \leq 0.2$ in Figure 15 just show a trend expected for $D(\Phi_\alpha)$.

The dotted lines in Figure 15 show the change of D with Φ_α as predicted from eqs 5 and 7 for the case when the two copolymers α and β are mixed molecularly to form a single microdomain morphology. It should be noted that the trend of D in the composition range of the miscible regime shown by eq 8 is *not consistent* with the $^2/_3$ power law relevant to the pure block copolymers and their mixtures miscible at all compositions.[29] D_α in the composition range of the miscible regime shows larger values than that predicted by eqs 5 and 7. There might be a possibility that the trend of D in the miscible regime of the partially miscible mixtures obeys a power law of a different kind of average molecular weight. This problem deserves a future work.

The fact that the smaller value of D_β hardly increases with increasing Φ_α implies that only a very small amount of α is solubilized into the macrophases rich in β with the smaller domain spacing. Equation 10 implies that the cost of free energy associated with the loss of conformational entropy of the block chains in the microdomain space may be greater in the case where α is solubilized in

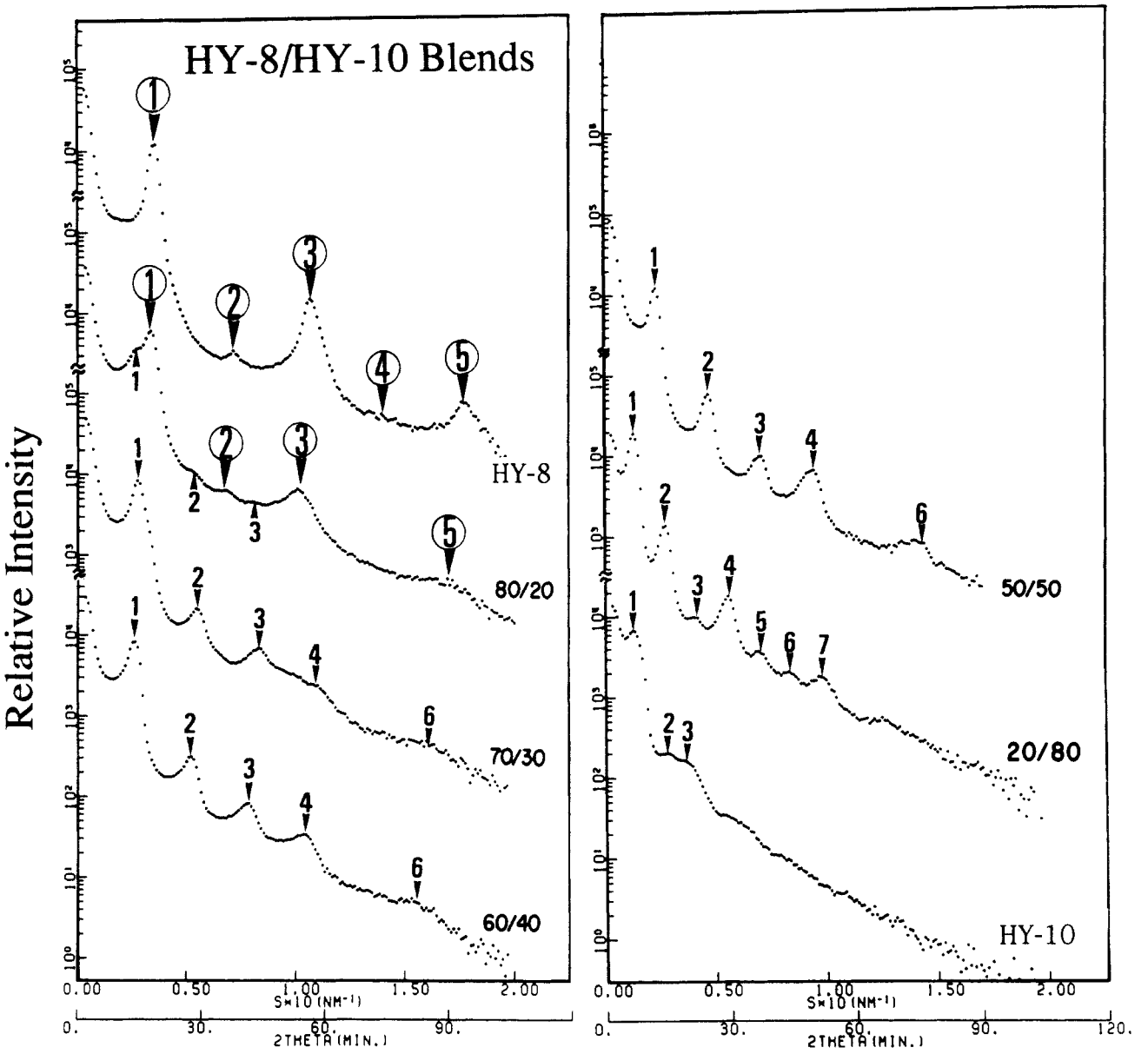

Figure 12. SAXS profiles obtained for the binary mixtures of HY-8/HY-10 with the compositions of 100/0 (wt %/wt %), 80/20, 70/30, 60/40, 50/50, 20/80, and 0/100. Scattering peaks due to the lamellae rich in HY-8 are indicated by numbers with circles, while the other peaks and shoulders indicated by numbers without circles are due to the lamellae rich in HY-10. Only pure HY-10 shows the scattering profile of OBDD-tetrapod. The number indicates the order of diffraction.

the β domain (Figure 16a) than in the case where β is solubilized in the α domain (Figure 16b). In any case the experimental results suggest that two copolymers α and β do not show total miscibility if

$$N_\alpha/N_\beta > 10 \tag{11}$$

The results given by eq 9 imply that, for the mixtures having Φ_α satisfying eq 9, the amount of free energy lowering upon the microdomain formation ΔF_{domain} is greater in the case when α and β undergo the macrophase separation into the lamellae having spacing D_α and D_β (see the change from parts a and b of Figure 17) than in the case when α and β mix at molecular level to form a single lamellar microdomain with spacing D_m, satisfying

$$D_\alpha < D_m < D_\beta \tag{12}$$

(see the change from parts a–c of Figure 17). A key physical factor associated with ΔF_{domain} is believed to be the conformational entropy (or the elastic free energy of stretching) of the block chains in the domain space, because the copolymer chains are in the confined space, with their chemical junctions at the interface, and stretched normal to the interface. The results are important to understand the self-assembling mechanism and process encountered in the solution-cast process, which will be discussed in a companion paper.[39]

V. Concluding Remark

A miscibility criterion was found for binary mixtures of poly(styrene-*block*-isoprene) which exhibit the lamellar morphology in most of the cases. In the miscible regime we found eq 7 as a scaling law of the lamellar spacing or domain identity period D with number-average molecular weight of the mixtures M_n. Two block copolymers were found to become immiscible in the composition range of Φ_α for the larger molecular weight copolymer satisfying eq 9, when the copolymer molecular weights are largely different as given by eq 11. The miscibility criterion or the coexisting composition $\Phi_{\alpha,CS}$(<0.2) or $\Phi_{\alpha,CL}$ (≅0.7) (eq 9) is proposed to strongly depend on the conformational entropy of the block chains confined in space (Figure 16). In the cases where the copolymers α and β are miscible and form a single morphology and they have a mismatch in composition (i.e., $f_{\alpha,A} \neq f_{\beta,A}$), the minority copolymers were found to be very effective in changing the interface curvature of the microdomain formed by the majority

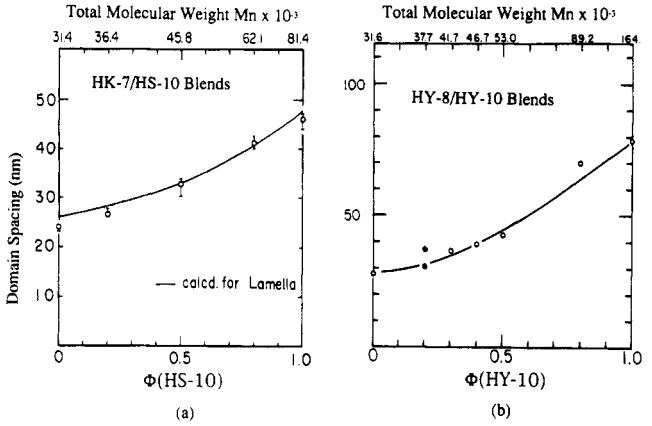

Figure 13. Plots of the average domain spacing against the weight fraction of the block copolymer with the larger molecular weight (α) for the binary mixtures showing a single morphology at all compositions. (a) HK-17/HK-10 mixtures. (b) HY-8/HY-10 mixtures. The solid curve is the theoretical prediction calculated for the lamellar microdomain.

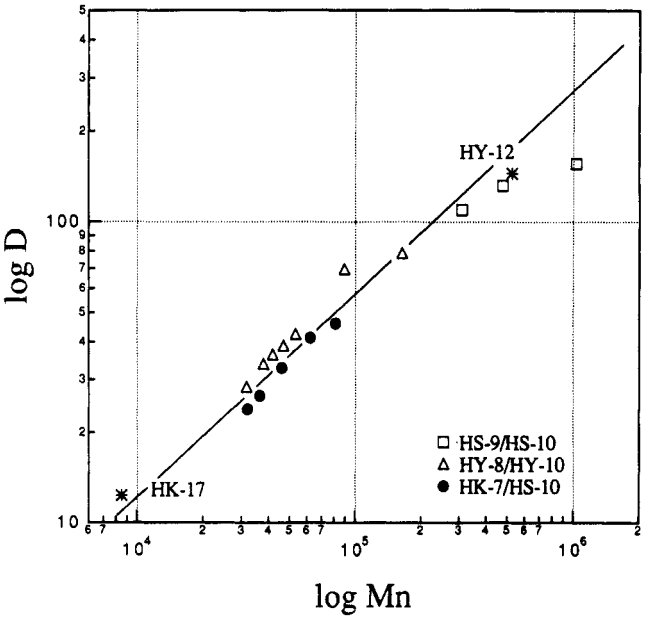

Figure 14. Double-logarithmic plot of the average domain spacing D against the number-average molecular weight M_n defined by eq 3 for the binary mixtures showing a single morphology. The results are consistent with the $^2/_3$ power law for pure block copolymers (solid line) except for the high molecular weight limit. The D value for HK-17 which corresponds to the wavelength of the dominant mode of the concentration fluctuations in the disordered state was also added in the figure as a reference.

copolymer. This curvature change causes the morphological transition from the lamellae to the ordered bicontinuous structure (parts a to b or c of Figure 4) or from the OBDD-tetrapod to lamellae (parts f to e of Figure 7) (*the curvature-driven morphological transition*). This curvature change is believed to be driven by free energy associated with packing the asymmetric copolymer chains ($f_{\alpha,A} \neq 0.5$ and/or $f_{\beta,A} \neq 0.5$) with $f_{\alpha,A} \neq f_{\beta,A}$ in the confined space. However one has to be cautious in the following point, in regards to the effect of the mismatch of the composition on the curvature change of the interface and hence on the curvature-driven morphological transition of the microdomain. If the mismatch becomes too large (though this is not the case in our system), the mean-field Flory interaction parameter χ_{eff} between α and β also becomes very large as predicted by eq 2. Under this condition, α and β undergo macrophase separation in the disordered state prior to the microphase separation, which

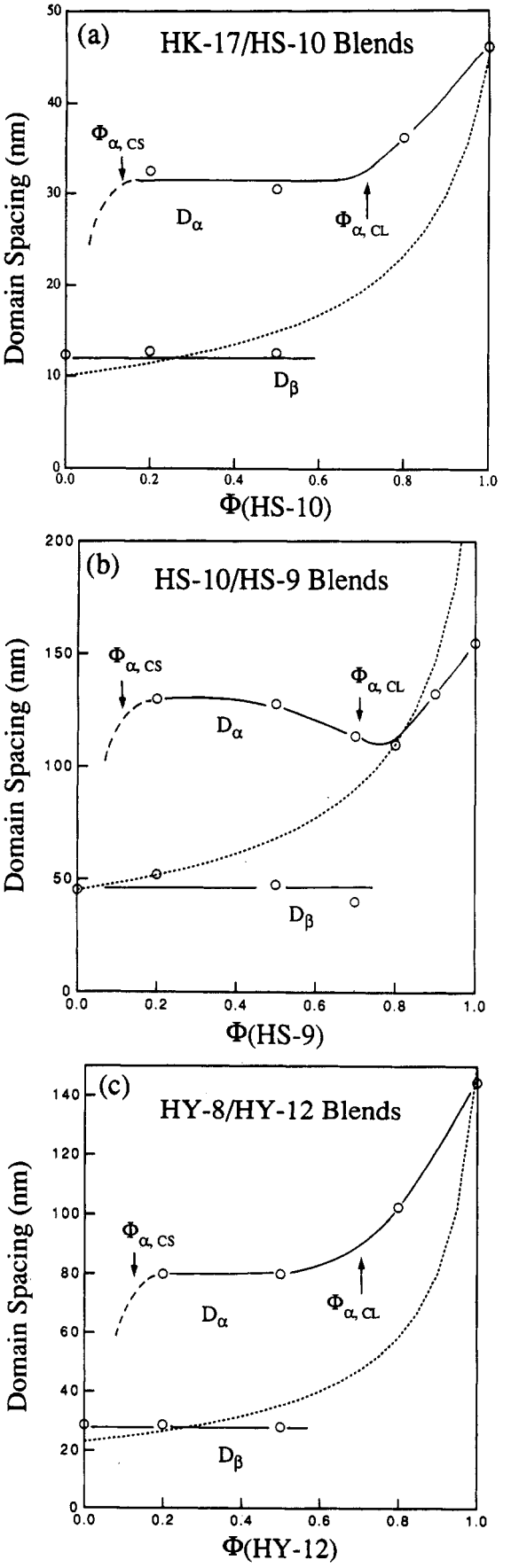

Figure 15. Plots of the average domain spacing against the weight fraction of the block copolymer with the larger molecular weight (solid lines) for the binary mixtures (a) HK-17/HS-10, (b) HS-10/HS-9, and (c) HY-8/HY-12. The mixtures show partial miscibility forming the two coexisting macrophases of the lamellae with large and small spacings, D_α and D_β, in the composition range between the critical concentration $\Phi_{\alpha,CS}$ and $\Phi_{\alpha,CL}$. The dotted curves are drawn according to the $^2/_3$ power law ($D = 0.025M_n^{2/3}$, $0.021M_n^{2/3}$, and $0.023M_n^{2/3}$ nm for a–c, respectively).

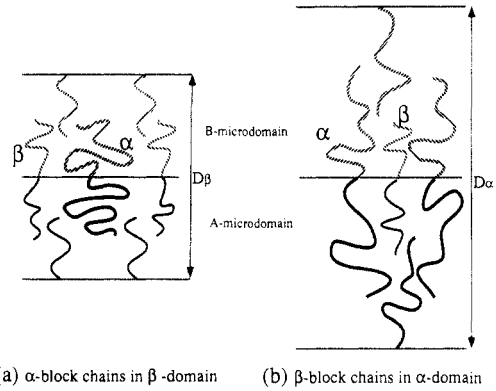

Figure 16. Schematic diagrams showing two possible extreme cases for packing two block copolymers with different chain length: (a) block copolymer α is solubilized in β domain; (b) β is solubilized in α domain. Loss of conformational entropy of the block chains may be greater in case a than in case b.

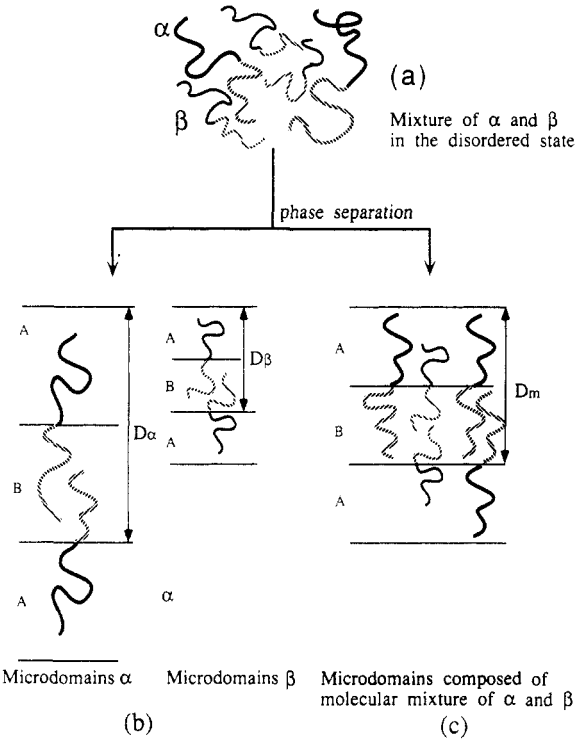

Figure 17. Summary of the possible ordered structures for the binary mixtures of block copolymers: (a) α and β mixed in the disordered state; (b) microdomain rich in α and microdomain rich in β coexisting; (c) single microdomain structure in which α and β are mixed in the microdomains.

completely alters the self-assembly and the final morphology[25,40] of the mixtures.

References and Notes

(1) Inoue, T.; Soen, T.; Hashimoto, T.; Kawai, H. *Macromolecules* **1970**, *3*, 87.
(2) Cohen, R. E.; Ramos, A. R. *Macromolecules* **1979**, *12*, 131.
(3) Zin, W.-C.; Roe, R.-J. *Macromolecules* **1984**, *17*, 189. Nojima, S.; Roe, R.-J. *Macromolecules* **1987**, *20*, 1866.
(4) Cohen, R. E.; Torradas, J. M. *Macromolecules* **1984**, *17*, 1101.
(5) Leibler, L.; Pincus, A. *Macromolecules* **1984**, *17*, 2922.
(6) Gebizlioglu, O. S.; Argon, A. S.; Cohen, R. E. In *Multicomponent Polymer Materials*; Paul, D. R., Sperling, L. H., Eds.; Advances in Chemistry Series 211, American Chemical Society, Washington, DC, 1986; p 259.
(7) Quan, X.; Gangarz, I.; Koberstein, J. T. *J. Polym. Sci., Polym. Phys.* **1987**, *25*, 641. Quan, X.; Gangarz, I.; Koberstein, J. T.; Wignall, G. D. *Macromolecules* **1987**, *20*, 1431.
(8) Tanaka, H.; Hoshimoto, T. *Polym. Commun.* **1988**, *29*, 212. Hashimoto, T.; Tanaka, H.; Hasegawa, H. In *Molecular Conformation and Dynamics of Macromolecules in Condensed Systems*; Nagasawa, M., Ed.; Elsevier: Amsterdam, The Netherlands, 1988; p 257.
(9) Berney, C. V.; Cheng, P.-L.; Cohen, R. E. *Macromolecules* **1988**, *21*, 2235. Cheng, P.-L.; Berney, C. V.; Cohen, R. E. *Macromol. Chem.* **1989**, *190*, 589.
(10) Kinning, D. J.; Winey, K. I.; Thomas, E. L. *Macromolecules* **1988**, *21*, 3502. Kinning, D. J.; Thomas, E. L.; Fetters, L. J. *J. Chem. Phys.* **1989**, *90*, 5806.
(11) Leibler, L. *Makromol. Chem., Macromol. Symp.* **1988**, *16*, 1.
(12) Owens, J. N.; Gangarz, I. S.; Koberstein, J. T.; Russell, T. P. *Macromolecules* **1989**, *22*, 3380, 3388.
(13) Winey, K. I.; Thomas, E. L. In *Material Research Society Symposium Proceedings*; Schaefer, D. W., Mark, J. E., Eds.; Material Research Society: Pittsburgh, PA, 1990; Vol. 171, p 255.
(14) Tanaka, H.; Hasegawa, H.; Hashimoto, T. *Macromolecules* **1991**, *24*, 240. Hashimoto, T.; Tanaka, H.; Hasegawa, H. *Macromolecules* **1991**, *24*, 5398, 5713. Koizumi, S.; Hasegawa, H.; Hashimoto, T. *Makromol. Chem., Macromol. Symp.* **1992**, *62*, 75.
(15) Hasegawa, H.; Tanaka, H.; Hashimoto, T.; Han, C. C. *J. Appl. Crystallogr.* **1991**, *24*, 672.
(16) Shull, K. R. *J. Chem. Phys.* **1991**, *94*, 5723.
(17) Winey, K. I.; Thomas, E. L.; Fetters, L. J. *Macromolecules* **1991**, *24*, 6182.
(18) Winey, K. I.; Thomas, E. L.; Fetters, L. J. *Macromolecules* **1992**, *25*, 422.
(19) Hashimoto, T.; Koizumi, S.; Hasegawa, H.; Izumitani, T.; Hyde, S. T. *Macromolecules* **1992**, *25*, 1443.
(20) Han, C. D.; Baek, D. M.; Kim, J.; Kimishima, K.; Hashimoto, T. *Macromolecules* **1992**, *25*, 3052.
(21) Hong, K. M.; Noolandi, J. *Macromolecules* **1985**, *18*, 2486.
(22) Shulz, A. R.; Berch, B. M. *Appl. Polym. Sci.* **1977**, *21*, 2305.
(23) Ijichi, Y.; Hashimoto, T. *Polym. Commun.* **1988**, *29*, 135.
(24) Tucker, P. S.; Barlow, J. W.; Paul, D. R. *Macromolecules* **1988**, *21*, 1678, 2794, 2801.
(25) Hashimoto, T.; Kimishima, K.; Hasegawa, H. *Macromolecules* **1991**, *24*, 5704.
(26) Milner, S. T.; Witten, T. A.; Cates, M. E. *Europhys. Lett.* **1988**, *50*, 413. Milner, S. T.; Witten, T. A.; Cates, M. E. *Macromolecules* **1988**, *21*, 2610. Milner, S. T.; Witten, T. A.; Cates, M. E. *Macromolecules* **1989**, *22*, 853.
(27) Birshtein, T. M.; Liatskaya, Yu. V.; Zhulina, E. B. *Polymer* **1990**, *31*, 2185.
(28) Hadziioannou, G.; Skoulios, A. *Macromolecules* **1982**, *15*, 267.
(29) Hashimoto, T. *Macromolecules* **1982**, *15*, 1548.
(30) Kim, J. K.; Kimishima, K.; Hashimoto, T. *Macromolecules* **1993**, *26*, 125.
(31) Fujimura, M.; Hashimoto, T.; Kawai, H. *Mem. Fac. Eng., Kyoto Univ.* **1981**, *43*, 224.
(32) Hendricks, R. W. *J. Appl. Crystallogr.* **1972**, *5*, 315.
(33) Mori, K.; Hasegawa, H.; Hashimoto, T. *Polym. J.* **1985**, *17*, 799.
(34) Hasegawa, H.; Hashimoto, T.; Hyde, S. T., to be submitted to *Macromolecules*.
(35) Hasegawa, H.; Tanaka, H.; Yamasaki, K.; Hashimoto, T. *Macromolecules* **1987**, *20*, 1651.
(36) Thomas, E. L.; Alward, D. B.; Kinning, D. J.; Martin, D. C.; Handlin, D. L., Jr.; Fetters, L. J. *Macromolecules* **1986**, *19*, 2197.
(37) Helfand, E.; Wasserman, Z. R. *Macromolecules* **1978**, *11*, 960.
(38) Shibayama, M.; Hashimoto, T.; Hasegawa, H.; Kawai, H. *Macromolecules* **1983**, *16*, 1427. Hashimoto, T.; Shibayama, M.; Kawai, H. *Macromolecules* **1983**, *16*, 1093. Shibayama, M.; Hashimoto, T.; Kawai, H. *Macromolecules* **1983**, *16*, 1434. Mori, K.; Hasegawa, H.; Hashimoto, T. *Polymer* **1990**, *31*, 2368.
(39) Part 2 of this series: Hashimoto, T.; Koizumi, S.; Hasegawa, H., in preparation.
(40) Part 3 of this series: Koizumi, S.; Hasegawa, H.; Hashimoto, T. in preparation.